High-resolution SH wave exploration to assess damage to the Sakuradani Kofun Tumulus No.2 caused by the Noto earthquake

Y. Hara[1], and R. Kuwano[2]

[1]Student, The University of Tokyo, Tokyo, Japan, email: yutarohr@iis.u-tokyo.ac.jp

[2]Professor, Institute of Industrial Science, The University of Tokyo, Tokyo, Japan, email: kuwano@iis.u-tokyo.ac.jp

ABSTRACT

Kofun, ancient Japanese burial mounds, are representing sophisticated geotechnical structures from ancient Japan. However, archaeological investigations of these heritage sites are often strictly restricted. Following the 2024 Noto Peninsula Earthquake, damage was observed in the Sakuradani Kofun Tumuli, including a subsidence (approx. 1.2 m diameter, 6.4 m length at 34.7° slope) confirmed in Tumulus No. 2. To aid restoration planning, this study assesses the subsurface damage in Tumulus No. 2 using non-invasive methods. Given the depth limitations of Ground Penetrating Radar (GPR), a Shear-Wave (SH-wave) reflection survey was selected to investigate the internal structure, focusing on the delineation of potential cavities and loose zones associated with the subsidence. A custom low-power vibratory source was utilized to minimize physical impact on the mound, employing waveform stacking to secure sufficient signal quality. The obtained seismic reflection profiles, interpreted alongside Dynamic Cone Penetration Test (DCPT) data, indicated reflectors corresponding to the dense foundation layer. Furthermore, hyperbolic reflections and amplitude attenuation were observed, which appear consistent with the presence of subsurface voids and associated loosened areas. These findings suggest that SH-wave reflection surveys can be an effective approach for the high-resolution, non-destructive assessment of structural damage in earthen heritage sites.

Keywords: Cavity detection, Non-destructive testing (NDT), Tumulus

INTRODUCTION

Japanese burial mounds, known as Kofun, are widely recognized as valuable historical heritage sites that convey the political culture of ancient times (Aoki, 2010). They are also complex geotechnical structures that aggregate ancient civil engineering technologies, ranging from tumulus specifications and slope angles to the selection of soil and construction of embankments. However, archaeological investigations of these heritage sites are often strictly limited. Therefore, methodologies that maximize results with limited time and resources are required. It is considered important to integrate archaeological knowledge, which predicts the location and shape of remains from historical contexts, with advanced expertise in subsurface exploration.

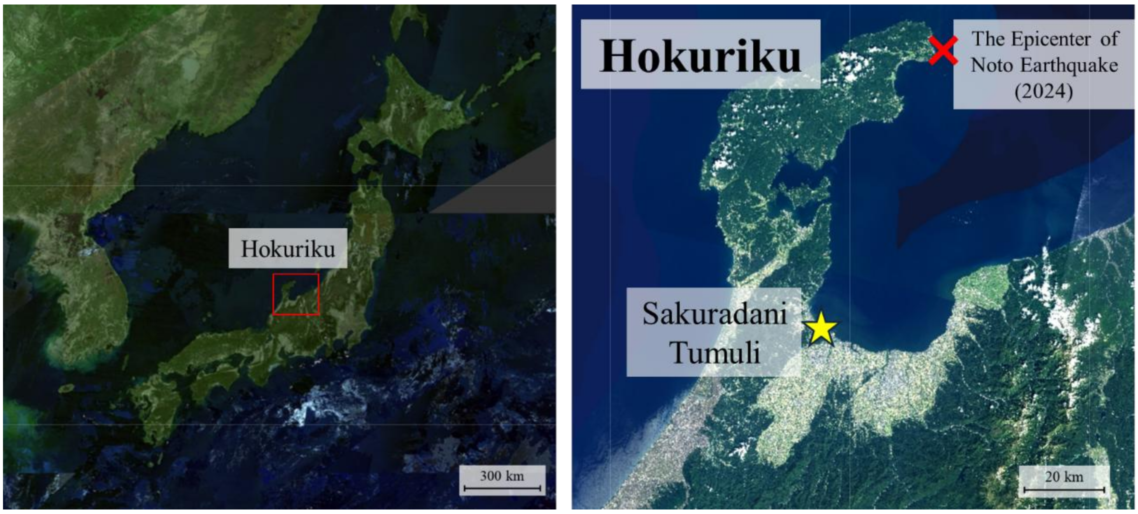

***Figure 1.** The Location of Sakuradani Kofun Tumuli (Base map source: Geospatial Information Authority of Japan, CC BY 4.0)*

Many Kofun, constructed over 1,300 years ago, are exposed to threats from natural disasters. For restoration and conservation, it is necessary to rapidly and accurately assess the extent of the damage to mitigate further deterioration. The 2024 Noto Peninsula Earthquake, a major inland event (M7.6) occurring at a depth of 16 km, caused damage to the Sakuradani Burial Mounds, located approximately 83 km from the epicenter (see Figure 1). The seismic intensity recorded near the site resulted in significant structural distress. In Tumulus No. 2, the subject of this study, a large-scale subsidence was observed following the earthquake, measuring approximately 1.2 m in diameter and 6.4 m in length, extending downward at a 34.7-degree slope, as shown in Figure 2.

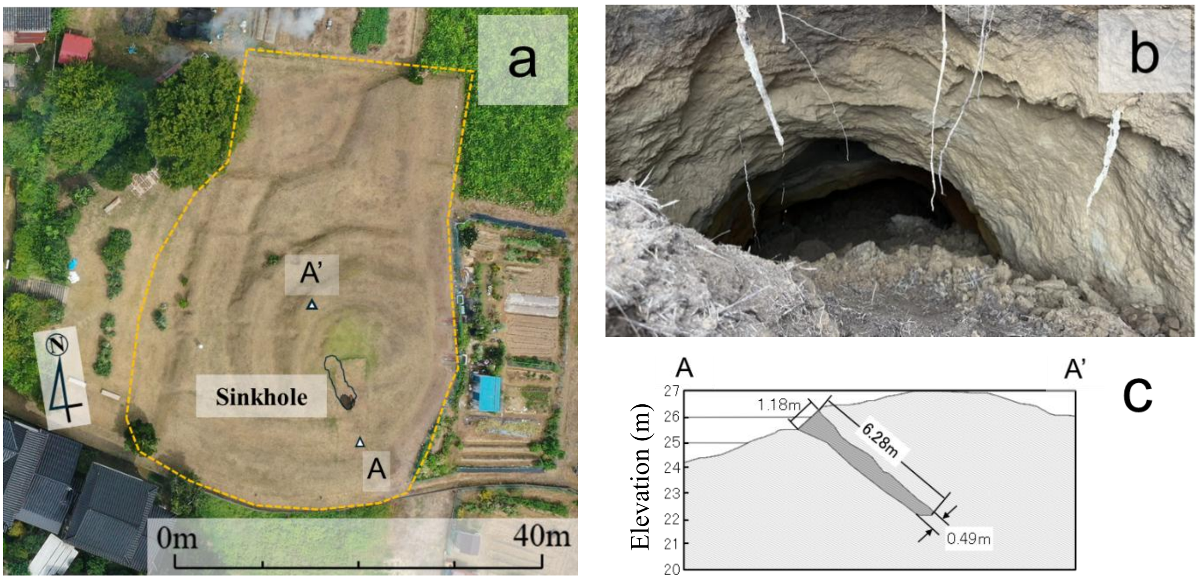

***Figure 2. a:** Damage at Sakuradani Tumulus No. 2, **b:** Sinkhole, **c:** Cross-section of the sinkhole.*

The objective of this study is to assess the overall damage status within the tumulus with minimal invasion as the first step toward the restoration of Sakuradani Tumulus No. 2. Non-destructive geophysical methods are increasingly applied in cultural heritage conservation to allow for internal structural assessment without excavation (e.g., Forte & Pipan, 2008). While Ground Penetrating Radar (GPR) is commonly used, its exploration depth is often limited (e.g., approx. 1.5 m) due to electromagnetic wave attenuation in conductive soils. This limitation suggests that GPR may be insufficient for understanding the entire structure of the 6-meter-high tumulus.

Recent studies globally have indicated that seismic surveys can extend investigation depth and resolution beyond traditional methods. Forte & Pipan (2008) demonstrated that combining P-wave seismic tomography with GPR could help overcome radar’s shallow penetration limits. Polymenakos &

Tweeton (2017) utilized seismic traveltime tomography to reconstruct 3D subsurface structures of large tumuli in Greece, identifying zones of differing soil quality non-invasively.

Furthermore, recent research highlights the potential value of shear-wave (S-wave) seismic methods for high-resolution imaging in earthen heritage structures. Mecking et al. (2021) applied Shear-Horizontal (SH) wave reflection profiling to the 32-m-high Yığma Tepe mound in Turkey, mapping internal stratigraphy and detecting subsurface anomalies associated with damage. Such advanced S-wave techniques leverage strong impedance contrasts at cavity boundaries, potentially providing a wider exploration range and higher resolution in the shallow subsurface (Mecking et al., 2021b; Rusch et al., 2022). Based on these precedents, it was anticipated that an elastic wave survey—specifically an SH-wave reflection survey—would be an effective approach for this study. This survey was implemented in June 2025 to attempt to identify cavities and loosened zones within the tumulus using a composite non-destructive approach.

METHODOLOGY

SH-wave reflection surveys are considered particularly suitable for visualizing local anomalies in the shallow subsurface (e.g., within 10 m). While common P-wave surveys are effective for deep reflective layers such as faults, they often lack sufficient resolution for shallow targets. In contrast, S-waves propagate significantly slower than P-waves in soft sediments, resulting in shorter wavelengths. This characteristic allows for the potential identification of detailed structures and local anomalies even in near-surface regions. Previous studies have demonstrated this capability, such as identifying deformation structures and discontinuities above abandoned mines (Guy et al., 2003) and accurately detecting urban cavities using advanced imaging techniques (Zhang et al., 2021). Given the small survey scale of less than 10 m, it was inferred that a shallow reflection method using SH-waves (Shear Horizontal waves), generated by horizontal excitation perpendicular to the survey line, would be effective. Reflection seismology determines the position of subsurface reflectors based on the relationship between the two-way travel time of the reflected wave and the offset distance between the source and receiver. The product of density and propagation velocity, which governs the reflection coefficient, is called impedance. At an interface where the impedance contrast between two layers is large, reflected waves are typically captured prominently. Since the target Tumulus No. 2 contains a sinkhole and associated loosened regions, strong impedance contrasts are expected. In a water-free cavity, both S-wave velocity and density are nearly zero, while a loosened layer exhibits low velocity and low density. Thus, clear reflections are anticipated at the boundaries of cavities or loosened zones.

Data Acquisition

When conducting seismic surveys on cultural heritage sites, the impact of vibration on the structure must be considered. Tumulus No. 2 consists of fine-grained sand, requiring a particularly delicate approach to maintain its structural integrity. To address this, a custom artificial vibration source was developed using a vibration speaker capable of controlling the input wave at low power. The appearance of the vibrator and trace example are shown in Figure 3. This device aims to achieve a sufficient Signal-to-Noise (S/N) ratio through waveform stacking despite low vibration power, enabling field data acquisition while minimizing physical load on the tumulus. In the data processing stage, an improvement of 4.4 dB in the S/N ratio after stacking was confirmed, demonstrating that high-quality signals can be secured even with a low-power source.

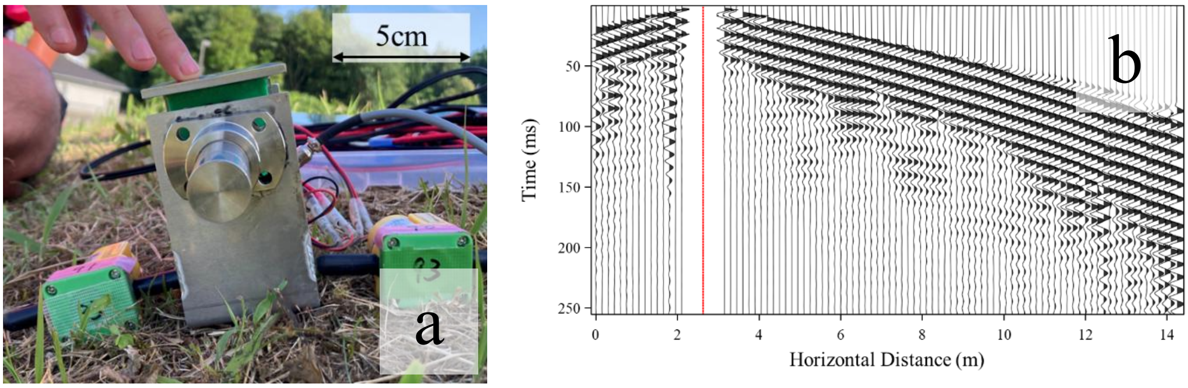

***Figure 3. a:** SH Vibrator **b**: Example of processed SH-wave seismograms. The waveforms were enhanced through bandpass filtering (60–150 Hz), stacking, and the application of Automatic Gain Control (AGC)*

The survey site was located approximately 50 m from a road with heavy traffic. The tumulus surface had vegetation of 10–20 cm, and the wind speed was approximately 10 m/s. To mitigate these external noises, waveform stacking was relied upon. Additionally, since SH-wave reflection analysis assumes a 2D cross-section, survey lines were selected to avoid gradients perpendicular to the line as much as possible. The locations of the survey lines on the tumulus are shown in Figure 4.

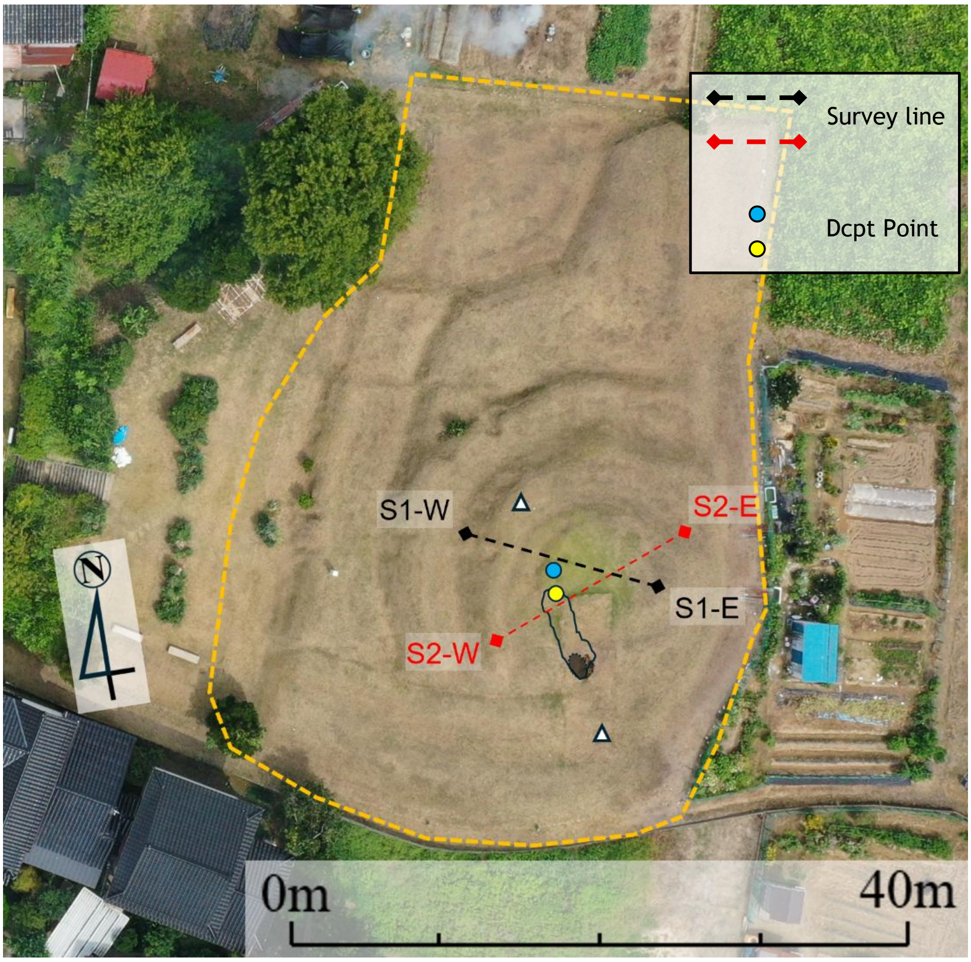

***Figure 4.** Location of Survey line1(S1) and line2(S2) on the Tumulus No.2*

For data acquisition, 96 SH-geophones with a natural frequency of 40 Hz were placed at 0.15 m intervals along two survey lines. The logger sampling frequency was set to 20 kHz, acquiring 8192 samples per trace. The estimated S-wave velocity of the surface layer was approximately 120–130 m/s.

The dominant frequency of the received waves was 85 Hz. The wavelength of the dominant wave was approximately 1.5 m. According to Rayleigh's 1/4 wavelength criterion, the vertical resolution is estimated to be about 0.4 m. This resolution is theoretically sufficient to identify the top and bottom surfaces of the observed sinkhole (approx. 1.2 m diameter, 6.4 m length, 34.7° slope, tip diameter 0.49 m), even considering projection effects.

Analysis

The processing and analysis of the acquired seismic data were conducted to visualize the internal structure of the tumulus. The workflow primarily consisted of (1) Pre-stack signal enhancement, (2) Common Midpoint (CMP) sorting, (3) Velocity analysis, and (4) Normal Moveout (NMO) correction with topographic adjustment, which removes the traveltime effect of source-receiver offset to flatten reflection events.

In the pre-stack processing phase, a bandpass filter of 60–150 Hz was applied to mitigate external noise. To enhance SH-wave components, horizontal vibrations perpendicular to the survey line were acquired in both forward and reverse directions. By subtracting one trace from the other, in-phase SH-wave components were emphasized while anti-phase P-wave components were suppressed. Given the low power of the custom vibrator, data was acquired twice in the same direction at each source point. These four datasets per point were stacked to improve the Signal-to-Noise (S/N) ratio. Following waveform synthesis, cross-correlation processing and Automatic Gain Control (AGC) were applied to reduce non-causal random noise and balance trace amplitudes.

Standard reflection seismic surveys typically assume a flat surface; however, the survey lines in this study were placed on a tumulus with significant relief. To address this, an NMO correction method applicable to rugged topography was introduced, adopting the approach described by Liu et al. (2005) to improve the accuracy of the reflection imaging.

The travel time difference Δt used for NMO correction, which accounts for elevation differences, is expressed as an equation (1):(Liu et al., 2005, p. 708 eq.9)

$$\Delta t = \sqrt{\frac{x^2}{v^2} + \left(t_0 + \frac{\Delta h_{sm} + \Delta h_{rm}}{v}\right)^2} - t_0 \tag{1}$$

where x is the offset, v is the velocity, t_0 is the zero-offset travel time, and Δh_{sm} and Δh_{rm} represent the elevation differences between the source-midpoint and receiver-midpoint, respectively.

Following the processing workflow described by Liu et al (2005), the coherence of the signals was evaluated for velocity estimation and stacking. We adopted the amplitude summation function based on the semblance measure defined by Neidell & Taner (1971), which is represented as (2):

$$A(t, v_s) = \sum_{j=0}^{K} \left(\sum_{i=1}^{N} s_i[t + v_s \Delta_t + j/F_s] \right) \tag{2}$$

Here, the optimum velocity spectrum was obtained by maximizing the stack energy by sweeping trial velocities v while scanning a time window. After NMO correction using the derived parameters, the reflection surfaces were stacked to generate the final analysis profile. Finally, to validate the seismic results, Dynamic Cone Penetration Tests (DCPT) were conducted at two points above the suspected cavity.

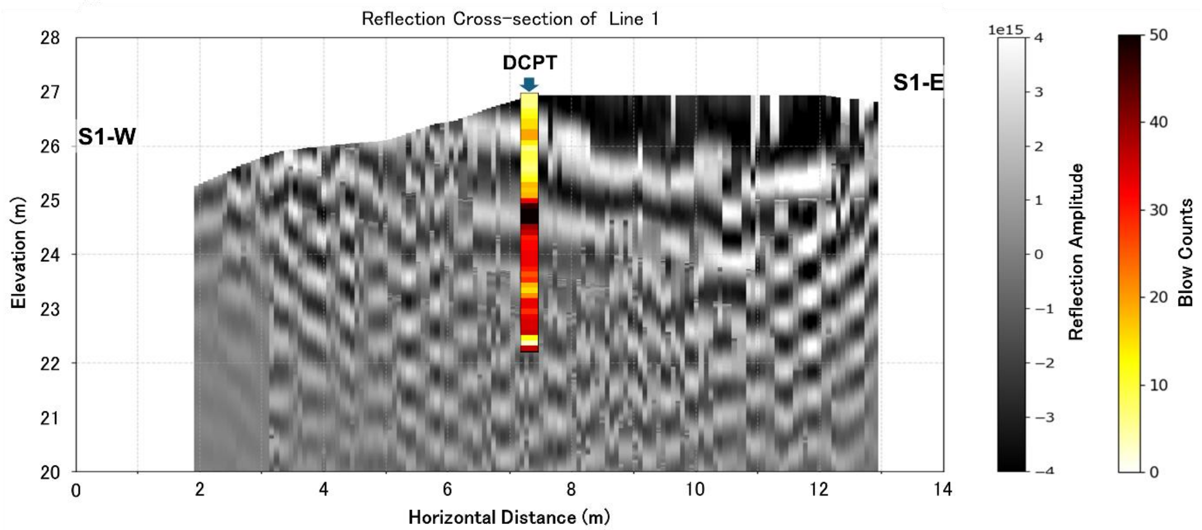

Figure 5. *Zero-offset SH-wave reflection profile for Survey Line 1. The locations of the Dynamic Cone Penetration Tests are indicated on the profile.*

RESULTS

Survey Line 1

The SH-wave reflection profile for Line 1 is shown in Figure 5. At DCPT Point 1, a boundary where the N_d value increases from 15 to 25 was observed at a depth of approx. 1.0 m, and a boundary where N_d increases from 15 to 48 was observed at approx. 2.1 m. Below 2.1 m, strata with $N_d > 50$ continued, indicating the presence of a dense embankment layer. However, layers exhibiting low strength ($N_d < 5$) appeared locally around 3.5 m and 5 m, suggesting soft soil layers intercalated within the tumulus.

In Line 1, vegetation with a thickness of approx. 0.2 m existed at the top of the tumulus, likely causing insufficient coupling of receivers to the ground, which resulted in relatively high noise levels and reduced S/N ratio in that section. Although the DCPT point is located about 0.5 m east of the survey line, causing some inevitable discrepancy, a positive high-amplitude reflection is recognized at the main depth of approx. 2.2 m. This is interpreted as a layer boundary consistent with the rapid increase in N-value in the DCPT. This boundary appears continuous from 6.6 m to 8.5 m along the line, but phase disturbance increases in the 8.5–10 m section, and the continuity of linear reflections decreases below this.

Furthermore, a strong reflection zone with high continuity is observed at an elevation of 24.8–25.0 m, cantered on the 6–10 m section of the profile. This zone shows a trend of gently deepening from west to east. A second reflection zone is distributed at an elevation of 23.2–23.6 m, and weak-to-moderate amplitude reflections are distributed in the shallow part at 25.6–26.2 m. Note that a near-surface velocity of 128 m/s was applied for depth conversion; if the true velocity is lower, systematic errors estimating the reflection depth shallower may occur.

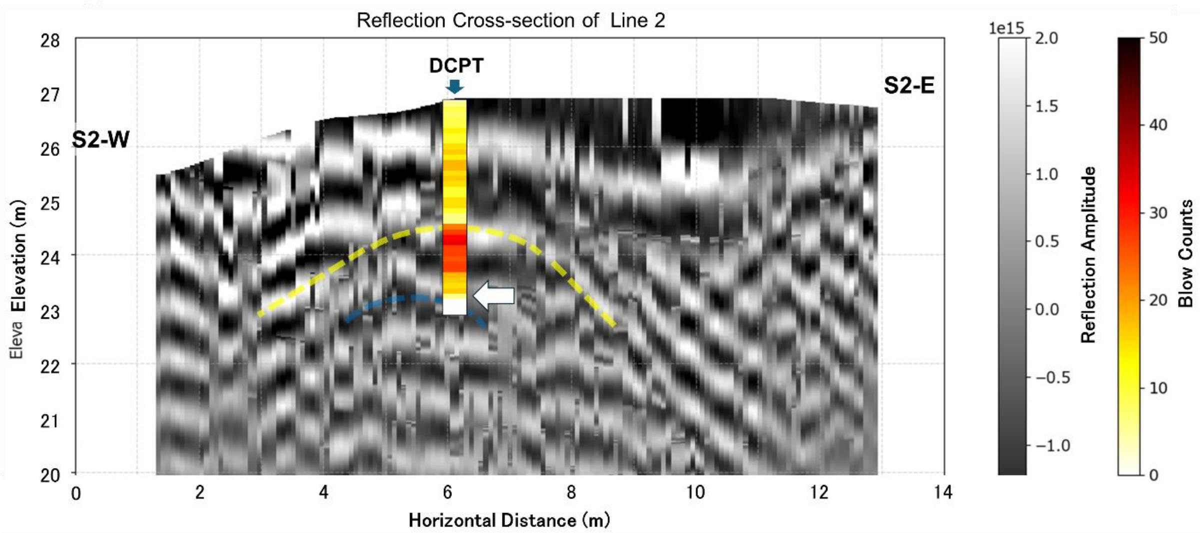

Figure 6. *Zero-offset SH-wave reflection profile for Survey Line 2. The locations of the Dynamic Cone Penetration Tests are indicated on the profile. The cavity boundary is highlighted by white arrows.*

Survey Line 2

The SH-wave reflection profile for Line 2 is shown in Figure 6. At DCPT Point 2, the penetration resistance dropped instantaneously by 30 cm at a depth of 3.5 m, suggesting the existence of a local cavity. While the N_d value was approx. 5–10 at depths of 0–2 m, it increased rapidly to $N_d > 30$ around 2.3 m depth, making the boundary to the dense layer clear. The cavity is estimated to be located at a depth of 3.5 m–3.8 m.

The SH-wave reflection profile of Line 2 is generally consistent with the major layer boundaries identified by DCPT. First, a continuous strong reflection band is observed around 2 m, where the transition to the hard layer was detected, indicating a boundary with a large impedance contrast. This reflection surface shallows from the west side (3 m point) to the 4.8 m point, forms a convex hyperbolic shape over approximately 2 m from 4.8 m to 6.8 m, and then deepens eastward from the 6.8 m point.

Around the cavity position at 3.5 m depth, a hyperbolic reflection surface was captured. Below this reflection surface, the reflection amplitude attenuates significantly, and a discontinuous zone with disturbed phases appears. This suggests the possibility of a cavity or an associated loosened region existing around the 5 m and 7 m points on the survey line.

CONCLUSION

This study conducted a high-resolution SH-wave reflection survey to assess internal damage to the Sakuradani Tumulus No. 2 caused by the 2024 Noto Peninsula Earthquake. By utilizing a custom low-power vibrator and waveform stacking techniques, seismic profiles were successfully acquired without imposing a significant physical load on the heritage site.

The results revealed continuous reflection bands corresponding to the boundaries between soft and dense layers, which correlated closely with N-value increments observed in DCPT profiles. Notably, in Line 2, hyperbolic reflections and subsequent signal attenuation facilitated the identification of subsurface anomalies. While it is technically challenging to definitively distinguish between air-filled cavities and extremely loosened soil zones based solely on seismic reflection characteristics—as both phenomena induce significant impedance contrasts—both features represent critical structural anomalies from a geotechnical conservation perspective. Consequently, this study categorizes these detected areas as "high-risk zones" that threaten the tumulus's stability. The SH-wave reflection survey thus proves to be an effective screening tool for identifying these potential hazards, even where a precise distinction between a void and loose soil remains subtle.

These findings align with previous studies (e.g., Mecking et al., 2021a) and suggest that SH-wave reflection surveys, when adapted for complex topography and heritage constraints, provide a robust, non-destructive basis for the restoration planning of ancient earthen structures.

ACKNOWLEDGEMENTS

We would like to express our gratitude to Takaoka City and Dr. Mai Sawada for the opportunity to conduct this field survey.

REFERENCES

Aoki, H. (2010). An analytical study on construction techniques of tombs through geoarchaeology: Focusing on tombs subjected to geotechnical investigation [Translated from Japanese]. Bulletin of the Graduate Division of Letters, Arts and Sciences of Waseda University. 4, 56, 79–95.

Forte, E., & Pipan, M. (2008). Integrated seismic tomography and ground-penetrating radar (GPR) for the high-resolution study of burial mounds (tumuli). Journal of Archaeological Science, 35(9), 2614–2623.

Liu, J., Xia, J., Chen, C., & Zhang, G. (2005). Accurate elevation and normal moveout corrections of seismic reflection data on rugged topography. New Zealand Journal of Geology and Geophysics, 48(4), 707–716.

Mecking, R., Köhn, D., Meinecke, M., & Rabbel, W. (2021a). Cavity detection by SH-wave full-waveform inversion – A reflection-focused approach. Geophysics, 86(3), WA123–WA134.

Mecking, R., Meinecke, M., & Pirson, F. (2021b). The Yığma Tepe of Pergamon: Internal construction of a monumental burial mound from shear wave reflection sounding and wavefield modelling. Archaeological Prospection, 28(4), 1–29.

Neidell, N. S., & Taner, M. T. (1971). Semblance and other coherency measures for multichannel data. Geophysics, 36(3), 482–497.

Polymenakos, L., & Tweeton, D. (2017). Non-invasive characterization of a burial tumulus with use of seismic P-wave velocity and attenuation tomography. Journal of Archaeological Science: Reports, 13, 36–48.

Rusch, K., Köhn, D., Stümpel, H., Gauß, W., & Rabbel, W. (2022). Prehistoric chamber tombs or geological pitfall? A multimethod case study from Ancient Aigeira with a focus on seismic full-waveform inversion. Archaeological Prospection, 29(1), 45–68.

Guy, E. D., Nolen-Hoeksema, R. C., Daniels, J. J., & Lefchik, T. (2003). High-resolution SH-wave seismic reflection investigations near a coal mine-related roadway collapse feature. *Journal of Applied Geophysics*, 54(1), 51–70.

Zhang, J., Liu, S., Yang, C., Liu, X., & Wang, B. (2021). Detection of urban underground cavities using seismic scattered waves: a case study along the Xuzhou metro line 1 in China. *Near Surface Geophysics*, 19(1), 95–107.